Seismic Risk and Environmentally Friendly Solutions: The Geotechnical Point of View

Maria Rossella Massimino[1(✉)] , Glenda Abate[1] , Angela Fiamingo[1] ,
and Dimitris Pitilakis[2]

[1] Department of Civil Engineering and Architecture, University of Catania, Via Santa Sofia 64, 95125 Catania, Italy
maria.massimino@unict.it
[2] Department of Civil Engineering, Aristotle University of Thessaloniki, P.O. BOX 424, 54124 Thessaloniki, Greece

Abstract. Over the past 50 years, there has been a tremendous growth in research in the field of seismic geotechnical engineering, producing very valuable results and highlighting the decisive role of the soil filter effect and soil-structure interaction in evaluating structural seismic risk. However, the challenge in assessing and mitigating seismic risk is not entirely over, with the continual opening up of new scenarios. A need to safeguard the ecosystem is encouraging researchers to find new solutions that combine seismic risk mitigation and ecosystem protection. Soil-rubber mixtures (SRM) have emerged as a new technique to improve the soil underneath foundations, so that seismic energy will be partially dissipated within the SRM. The rubber grains are manufactured from scrap tyres, disposal of which has become a severe environmental problem worldwide. SRMs are characterized by low specific weight, high elasticity, low shear modulus, and high damping. The present paper reports some interesting results obtained by the authors as regards seismic microzonation, local site response, and soil-structure interaction. Finally, the paper reports the main results of the first tests performed on a full-scale soil-SRM-structure system and a FEM simulation of these tests.

Keywords: Local site response · Dynamic soil-structure interaction · Geotechnical seismic isolation · Scrap tires · Full-scale tests · FEM modelling

1 Introduction

As demonstrated by an analysis of the damage caused by many earthquakes, the first fundamental steps to be taken towards a realistic seismic design of new structures and seismic retrofitting of existing ones are an investigation of the soil filter effect and the complex soil-structure interaction phenomena. Reducing the seismic risk of structures and infrastructures is still an environmental challenge that has not been thoroughly addressed. In all parts of the world, the soil filter effect is computed by means of free-field (FF) local site response (LSR) analyses [1–3]. This approach represents a significant step forward compared to the use of the response acceleration spectra furnished by technical codes.

LSR considers the specific conditions of the subsoil (geometry, physical properties, non-linearity) and, therefore, its fundamental filtering effect in terms of PHA, PHV, PHD, predominant frequencies, Arias intensity, and so on [4–8]. It allows us to develop seismic microzonation maps for a rational use of the territory and to appropriately estimate the seismic inputs that affect structures and infrastructures.

Nevertheless, the dynamic response at the foundation level of structures can significantly deviate from the FF site response due to kinematic and inertial interaction [9–22], and in some cases, the Dynamic Soil-Structure Interaction (DSSI) could be detrimental to the structures involved [23]. In this regard, experimental tests and numerical modelling of fully-coupled soil-structure systems are the most valuable approaches, in that they produce results that most nearly reflect the actual configurations. Moreover, in recent years, a need to safeguard the ecosystem has encouraged researchers to find new solutions that combine seismic risk mitigation and ecosystem protection. Among others [24–26], soil-rubber mixtures (SRM) have emerged as a new, valuable technique for protecting structures in earthquake-prone areas. The main idea is to improve the soil immediately underneath the foundations using SRMs so that seismic energy will be partially dissipated within the SRMs before being transmitted to the structures. Rubber grains for the mixtures are manufactured from scrap tyres, the disposal of which has become a severe environmental problem worldwide. SRMs are characterized by low specific weight, high elasticity, low shear modulus, and high damping. Experimental and numerical analyses have shown good performance of SRMs in static and dynamic conditions as geotechnical seismic isolation (GSI) solutions [27–34].

The present paper reports some interesting geotechnical works developed by the authors regarding seismic risk analysis and mitigation, including new eco-sustainable solutions. In particular, the paper reports the main results of:

i)   An extensive LSR analysis for the development of seismic microzonation maps in the city of Noto (south-eastern Sicily, Italy). These maps are fundamental for urban and spatial planning with the idea of sustainable development, including the reconstruction and renovation of historic buildings. Noto is famous worldwide for its unique Baroque cultural heritage, but is characterized by a very high seismic vulnerability in an area with medium-high seismicity.

ii) A DSSI analysis of a fully coupled soil-structure system regarding the strategic headquarters of the National Institute of Geophysics and Volcanology (INGV), Catania Section. The building is a valuable masonry structure, built at the end of the 1800s and characterized by a critical seismic vulnerability.

iii) The first experimental campaign on a full-scale prototype structure resting on gravel-rubber mixtures (GRM) and a FEM simulation of the same. Thus, the use of GRM underneath structures aims to provide a desirable new solution that combines seismic risk mitigation and ecosystem protection.

2 An Interesting Example of Seismic Microzonation

The reduction of seismic risk in urban areas is an environmental matter which should be approached starting from a careful evaluation of local seismic hazard. Several studies have been conducted in earthquake-prone areas to develop seismic microzonation maps. The authors present an interesting example regarding the city of Noto (south-eastern Sicily, Italy), famous worldwide for its Baroque cultural heritage.

In ancient times south-eastern Sicily was shaken by strong earthquakes that destroyed Augusta, Siracusa, and Noto and produced serious damage in Catania, all cities with a rich, historic and artistic heritage. The seismic history of this area has been marked by a few high-energy earthquakes, with eight very strong shocks occurring over the last nine centuries, all having an epicentral intensity in the VIII–XI MCS range. The last of these (VIII MCS) dates back to January 11th, 1846. The strongest earthquake to occur after this (VII-VII MCS), took place on December 13th, 1990, with an epicentre close to Augusta [35, 36].

As regards the city of Noto, it was destroyed by the earthquake that occurred on January 11th, 1693. It also sustained heavy damage during the one on January 7th, 1917. The most recent earthquake on December 13th, 1990, damaged several important buildings and highlighted the need to safeguard the city's valuable cultural heritage. The photographs on the left of Fig. 1 show a view of some important buildings in Noto and the cathedral, which partially collapsed as a result of the 1990 seismic event.
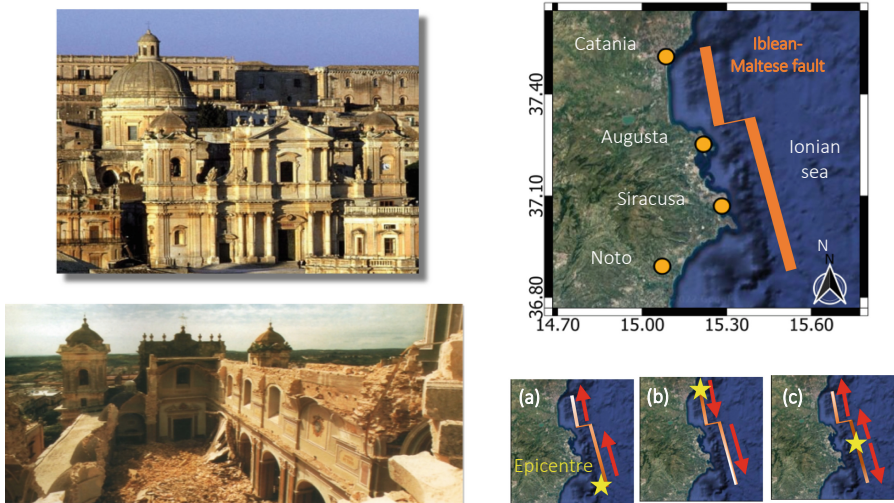

Fig. 1. On the left: a view of the valuable cultural heritage in Noto and the partial collapse of the cathedral due to the December 13th, 1990 earthquake; on the right: the rupture propagation models along the Iblean-Maltese fault used to compute the synthetic accelerograms for Noto. The star indicates the rupture nucleation.
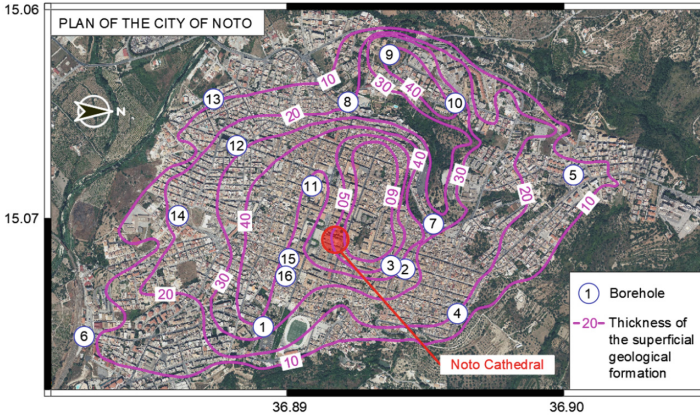
Fig. 2. Borehole location for the seismic microzonation of Noto.

Due to a lack of sufficient instrumental records, the seismic hazard of the area was established using synthetic accelerograms. Based on the geological and macroseismic observations of the 1693 earthquake, Bottari et al. [37] modelled the strong motion in Noto, considering the Iblean-Maltese fault (Fig. 1) as the seismogenic source of the target earthquake. More details can be found in [37]. Three different rupture propagating models were considered: a) a unilateral rupture from South to North; b) a unilateral rupture from North to South; c) a bilateral rupture. Then, synthetic accelerograms at the depths of 30 m and 70 m were computed for the E-W, N-S and vertical directions. The maximum PHA of the input motions, equal to 1.48 m/s^2 was related to rupture model 1 – E-W component, while the minimum, equal to 0.39 m/s^2, was related to rupture model 1 – N-S component. Of all the synthetic accelerograms, those at a depth of 30 m were used here because the in-situ tests performed for the whole of Noto showed that the conventional bedrock ($V_s \geq 800$ m/s) is located at variable depths of between approximately 9.00 m and 40.00 m (Figs. 2 and 3). The soil is mainly constituted by: talus material up to a depth equal to 13.00–15.00 m; sand and gravel at a depth equal to 2.00–25.00 m; clay-marly clay at a depth equal to 19.00–27.00 m and sand and silty clay up to a depth of 34 m. Laboratory tests also allowed the soil nonlinearity to be estimated [38].

The local seismic response was evaluated using the 1-D nonlinear GEODIN code [39], applying the input synthetic accelerograms at the conventional bedrock estimated for all the 16 boreholes in Fig. 2. The local seismic response was analyzed in terms of maximum horizontal acceleration, velocity and displacement at the soil surface ($a_{\text{max,surf}}$, $v_{\text{max,surf}}$, $d_{\text{max,surf}}$), as well as in terms of amplification ratio (R), which is the ratio between the maximum acceleration at the soil surface and the maximum acceleration at the bedrock. Response spectra at the soil surface were also computed. Based on the values of $a_{\text{max,surf}}$ and R for each geological zone determined by the curves reported in Fig. 2 different microzonation maps were drawn up. Due to a lack of space, only the microzonation map in terms of R, for the N-S component of the input synthetic

accelerograms related to source rupture model 1 is reported in this paper (Fig. 4) because it represents the most severe response in terms of R ($R = 2.73$–4.05).
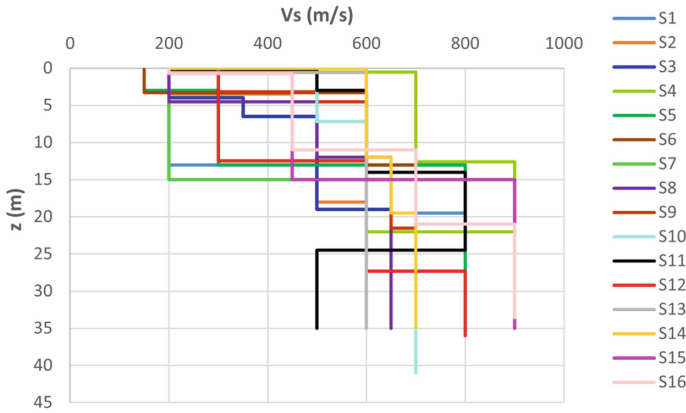

Fig. 3. V_S vs z profiles for all the boreholes reported in Fig. 2.

Globally, the most severe zones in terms of R are: a) the small area in which the thickness of the superficial geological formation is equal to or more than 40 m, where R varies between 1.70 (source rupture model 1 – E-W component) and 4.05 (source rupture model 1 – N-S component); b) the area characterized by a thickness of the superficial geological formation in the range of 20–30 m, where R varies from 1.18 (source rupture model 3 – N-S component) to 3.38 (source rupture model 1 – N-S component). The most severe response in terms of R is reached considering model 1 and the N-S component, for which the relative input synthetic accelerogram is characterized by the lowest peak value of amplitude but by a predominant period, equal to 0.15 s, which is very close to the natural vibration period of most of the soil profiles. This confirms, once more, the critical role played not only by the peak value of amplitude but also by the frequency content of the input accelerograms. More details can be found in [40].

3 From Local Site Response to Soil-Structure Interaction

In structural design/retrofitting, the design spectra and the ground motion acceleration time-histories are given by technical regulations or, more appropriately, derived by free-field (FF) local site response (LSR) analyses, such as that discussed in the previous section. The latter approach is a significant step forward, in that it considers the specific conditions of the subsoil. Nevertheless, the dynamic response at the foundation level of structures can deviate from the FF site response due to kinematic and inertial interaction and in some cases, the DSSI could be detrimental to the structures involved. In this section, the authors report a DSSI study performed in 2017 for the headquarters of the National Institute of Geophysics and Volcanology (INGV), Catania Section (Fig. 5a). The building and its subsoil were investigated during the POR-FESR Sicilia
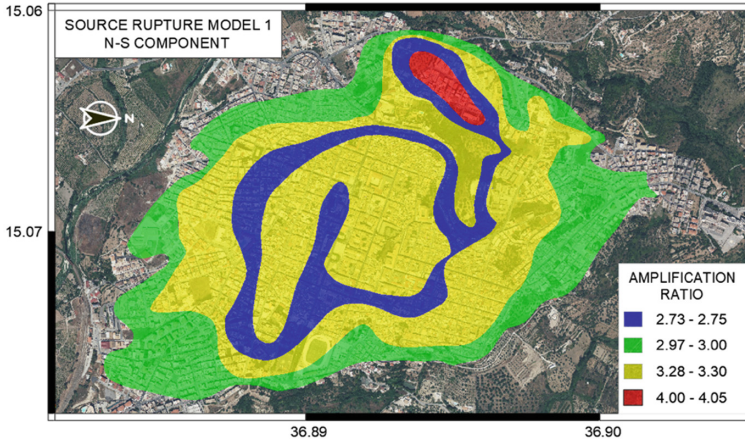
Fig. 4. Seismic microzonation map of Noto in terms of acceleration amplification ratio (*R*) using the synthetic accelerogram related to source rupture model 1 – N-S component.

2007–2013 research project, aimed at reducing seismic risk in Eastern Sicily. The seismic response of the fully-coupled system was investigated using a 2D FEM modelling (Fig. 6), considering soil-nonlinearity according to [41]. The results of the full-coupled system analyses (see the SSI alignment in Fig. 6) were compared with those related to the free-field site response (see the FF$_{left}$ and FF$_{right}$ alignments in Fig. 6) in the time and frequency domains in terms of soil amplification ratio, Fourier and response spectra, and amplification functions. The resulting soil amplification ratio and response spectra were also compared with those given by the Italian technical regulation in force in 2017 [42]. Finally, the maximum shear forces at each level of the structure were compared with those given by the fixed-base structure configuration, traditionally used in engineering practice. In the present paper, the authors report the main results in terms of acceleration amplification ratio (Fig. 7) and acceleration response spectra (Fig. 8). The other results are reported in [44].

The INGV building is a masonry structure built at the end of the 1800s, whose bearing walls are built of lava stone; the foundations are enlargements of these walls, and they are embedded to a depth equal to 2.5 m. The floors are in brick and concrete, downloading on curbs in reinforced concrete resting on the walls. The bedrock is more than 200 m below ground level as regards the soil. However, it was fixed at 40 m (conventional bedrock) for the FEM analyses presented here, according to previous 1D analyses, which showed no significant amplification from z = 200 m to z = 40 m. The soil is of class C according to [42]. The main geotechnical properties are summarized in Table 1. The values reported in the table were modified in the FEM analyses according to [41] to take soil-nonlinearity into account.

Seismic inputs were applied at the base of the FEM model. The inputs chosen were: six synthetic accelerograms evaluated assuming the source to be along the Hyblean-Maltese fault and generating the 1693 seismic ground motion scenario (1693(1), $f = 2.06$ Hz; 1693(2), $f = 2.31$ Hz, 1693(3), $f = 2.31$ Hz) and the 1818 seismic ground motion scenario (1818(1), $f = 0.66$ Hz; 1818(2), $f = 0.52$ Hz, 1818(3), $f = 0.58$ Hz); the
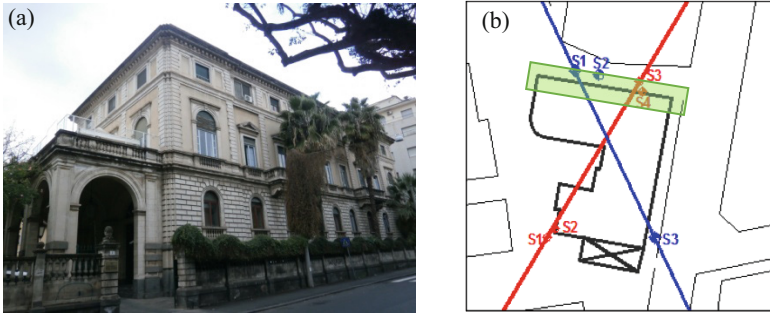
Fig. 5. a) View of the INGV building; b) plan view of the INGV building (in red the boreholes performed in 2010, in blue the boreholes performed in 2014, in green the section investigated with the 2D FEM analysis).

Table 1. Main geotechnical properties – INGV building case-history.

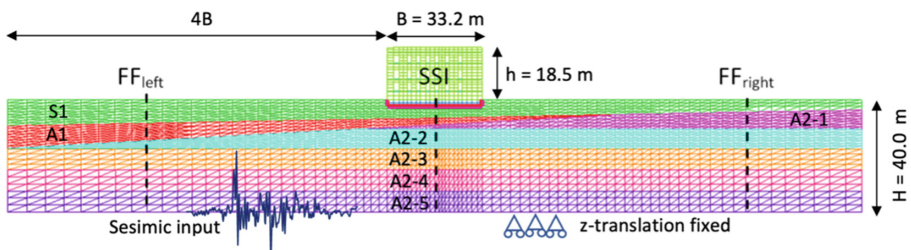| Layer	H (m)	V_s (m/s)	ν	ρ (t/m^3)	G_0 (kPa)	E_0 (kPa)
sandy silt (S1)	6.7	179	0.25	2.04	65363	163409
clay1 (A1)	2.8	193	0.25	2.01	74870	187176
clay2–1 (A2–1)	1.6	197	0.25	2.01	78006	195015
clay2–2 (A2–2)	6.6	222	0.25	2.01	99061	247652
clay2–3 (A2–3)	7.2	253	0.25	2.01	128658	321645
clay2–4 (A2–4)	7.2	277	0.25	2.01	154225	385563
clay2–5 (A2–5)	7.2	310	0.25	2.01	193161	482903

Fig. 6. FEM model of the 2D section of INGV building highlighted in green in Fig. 5b.

accelerogram recorded at the Sortino station during the 1990 earthquake ($f = 2.38$ Hz). To fit the accelerograms to the reference area, they were scaled at the same maximum expected acceleration (PHA = 0.282 g), corresponding to the SLV state (i.e. the limit state for the safety of human life) and considering the building as "strategic" type (corresponding to a return period of 975 years), in accordance with [42]. The synthetic

seismograms were also scaled using attenuation relations, considering the epicentral distances for both the earthquake scenarios. More details can be found in [44].

Figure 7 reports the amplification ratio R along the free-field alignments on the left (FF_{left}) and on the right (FF_{right}) and along the alignment crossing the structure (SSI), see also Fig. 6. Comparing the FF_{left} and FF_{right} alignment results, it is possible to observe some differences due to the different soil profiles. Comparing the results for both the FF and the SSI alignments, it is possible to observe a good agreement for the 1693 inputs, definitely greater R values along the SSI alignment for the 1818 inputs and lower values of R along the SSI alignment for the 1990 input. The different response in terms of R along the FF and SSI alignments depends on DSSI phenomena and the relation between the frequency content of the input applied at the base of the FEM model and the natural frequency of the system, equal to 0.94 Hz considering only the soil (FF alignments) and to 0.88 Hz including the building (SSI alignment). For the 1818 inputs, their predominant frequencies are closer to the natural frequency of the entire soil-building system, so the acceleration at the base of the building is higher than those in FF conditions. In the latter case, the DSSI is detrimental. Moreover, the amplification ratios computed are generally significantly higher than that suggested by [42], equal to 1.29.
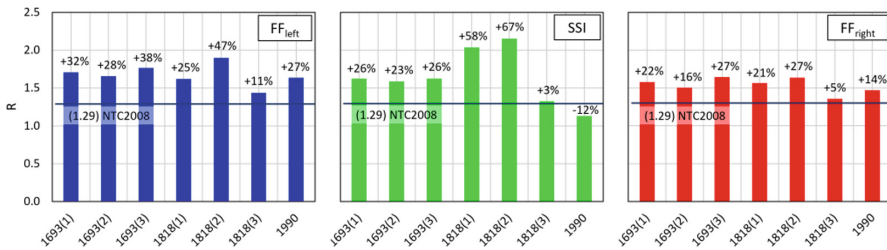

Fig. 7. Acceleration amplification ratio along the FF_{left}, SSI and FF_{right} alignments shown in Fig. 6 obtained with the FEM modelling compared to the value prescribed by NTC,2008.

Figure 8 shows the average response spectra at the soil surface obtained by the FEM-2D modelling and, in accordance with [42], for a structural damping ratio equal to 8%. It can be noticed that between the average spectra obtained for the free-field conditions (FF_{left} and FF_{right}), there are no substantial differences. On the contrary, a notable difference exists between the average response spectra obtained for the free-field conditions and that concerning the SSI alignment. The FF response spectra present the highest peak for $T = 0.42$ s and a second, less evident peak for $T = 1.27$ s, while the SSI response spectrum gives the highest peak for $T = 1.27$ s and a second, less noticeable peak for $T = 0.42$ s. The natural period of the structure, including the subsoil, is equal to 1.13 s. Thus, the SSI response spectrum indeed reports the most dangerous situation. In this case, the DSSI is detrimental, and neglecting it, would produce an unsafe design. It is also important to underline that the NTC2008 response spectrum [42] does not cover the computed SSI average response spectrum for periods greater than 0.7 s. The latter is often the period of structures on the subsoil (no fixed-base), which is the realistic configuration of structures.
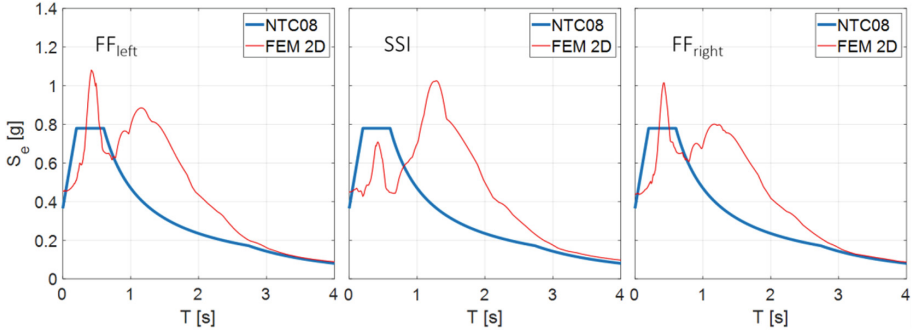
Fig. 8. Comparison of the average elastic response spectra obtained by the FEM analyses and that prescribed by [42] at the soil surface.

4 A New Eco-sustainable Geotechnical Solution for Reducing the Seismic Risk of Structures

To reduce the seismic energy transmitted to structures, new low-cost and eco-sustainable seismic isolation systems have been investigated, consisting of soil-rubber-mixtures (SRM) underneath the foundations. Seismic energy will be partially dissipated within this mixture before being transmitted to the structures.

The first experimental campaign on a full-scale prototype structure resting on gravel-rubber mixtures (GRMs) was performed in 2019 in Thessaloniki, Greece [45]. The Euro-Proteas prototype structure (Fig. 9a) was chosen for the experiment. This is a perfectly symmetric steel frame on a RC slab and supports two RC slabs. Steel X-braces connect the four steel columns in both directions. Over the last few years, many tests have been performed on this structure. More details can be found in [46–48]. In 2019, it was used within the framework of the European SOFIA-SERA project, after replacing the foundation soil with three different GRMs to a thickness of 0.5 m. The study investigated the rubber content effect of the GRM layer on the dynamic response of the EuroProteas structure and the overall performance of the GRMs as a geotechnical seismic isolation (GSI) system. Both free-vibration and forced-vibration tests were performed at different excitation levels, with and without rubberised soil underneath the foundation. This paper deals with the sets of forced-vibration tests.

The uppermost 0.5 m of the foundation soil was replaced with three different GRM backfills (Fig. 9b). The rubber content per mixture weight (p.w.) was fixed equal to 0%, 10%, and 30% for the three foundation mixtures labelled in the following as GRM 100/0, GRM 90/10, and GRM 70/30, respectively. The gravel used was characterized by $D_{50,G}$ = 20.76 mm and $G_{s,G}$ = 2.67. The rubber was recycled granulated rubber from car tyres characterized by $D_{50,R}$ = 3.27 mm, and $G_{s,R}$ = 1.10. Figure 10a shows their grain size curves. GRM 100/0 was characterized by $G_{s,G}$ = 2.67, D_r = 98%, γ_d = 16.2 kN/m^3; GRM 90/10 was characterized by $G_{s,G}$ = 2.51, D_r = 98%, γ_d = 15.2 kN/m^3; GRM 70/30 was characterized by $G_{s,G}$ = 2.19, D_r = 59–71%, γ_d = 11.8 kN/m^3. The three GRMs were located in three different 3.2 x 3.2 x 0.5 m square-plan pits. A thin geotextile layer was placed to cover the pit to prevent the GSI from mixing with the underlying

and surrounding fine-grained soil material. The GRM foundation soil was spread in two layers both 0.25 m in height. Each layer was compacted using a soil compactor.
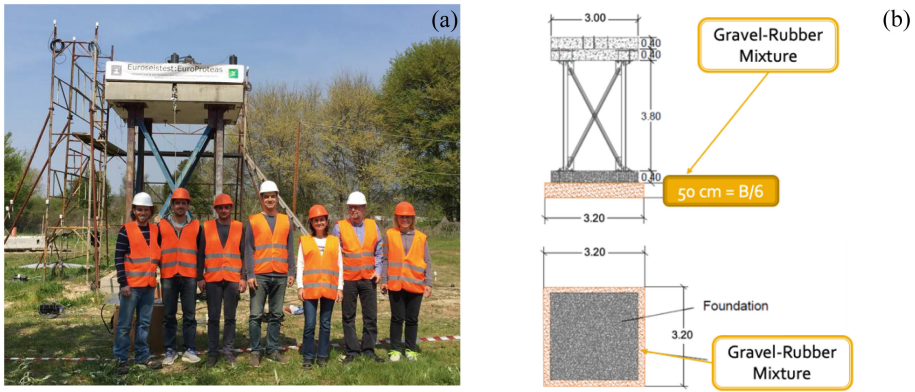

Fig. 9. a) View of the Europroteas structure and the team involved in the European SOFIA-SERA project [https://sera-ta.eucentre.it/sera-ta-project-40/]; b) Section and plan view of the Europroteas structure including the gravel-rubber mixture.
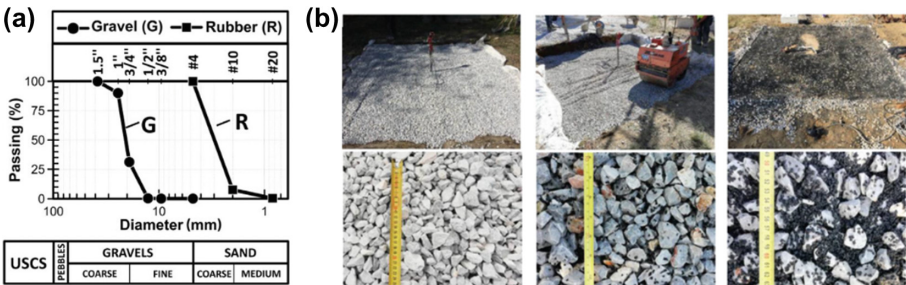

Fig. 10. a) Grain size distribution curves of the gravel and the rubber used in the full-scale tests; b) the soil pit filled with GRM100/0, GRM90/10 and GRM70/30 and details of the mixtures in each soil pit (modified by [45]).

The soil below the structure was investigated using extensive geotechnical and geo-physical surveys, including static and dynamic in-situ and laboratory tests [49]. The subsoil consisted of a 7 m thick upper layer of silty clayey sand, which overlay a layer of clayey to silty sand with gravels between 7 and 22 m and, after that, a layer of marly silt to silty sand up to a depth of 30 m. The shear wave velocity of the uppermost 5 m varied from 100 to 150 m/s and then increased to more than 250 m/s at a depth of 25 m (Fig. 11).

The input force was applied to the roof by an eccentric mass shaker. The eccentricity and the operating frequency adjusted the force amplitude according to the equation $F = E \cdot (2\pi f)^2$, where F is the shaker force (in N), E is the total eccentricity of the shaker (in kg-m), and f is the rotational velocity of the shaker (in Hz). Only the tests characterized by an eccentricity equal to 6.93 kg-m are shown here due to lack of space.

The structure was shaken for a time window of 25 s at each excitation frequency to reach a steady state. The input frequency range was 1–10 Hz. Ambient noise measurements made it possible to estimate the natural frequencies of the fixed-base structure (f_1 = 9.13 Hz) and the flexible-base structure resting on GRM 100/0 (f_1 = 4.4 Hz; f_2 = 4.9 Hz; f_3 = 9.7 Hz), GRM 90/10 (f_1 = 4.3 Hz; f_2 = 4.6 Hz; f_3 = 9.4 Hz), and GRM 70/30 (f_1 = 2.4 Hz; f_2 = 2.7 Hz; f_3 = 7.1 Hz). GRM 100/0 and GRM 90/10 led to very close natural frequencies, thus showing that a 10% rubber content is not so influential. The natural frequencies substantially decreased when changing from GRM 90/10 to GRM 70/30. As expected, the increase in the rubber content produced a reduction in the natural frequencies.
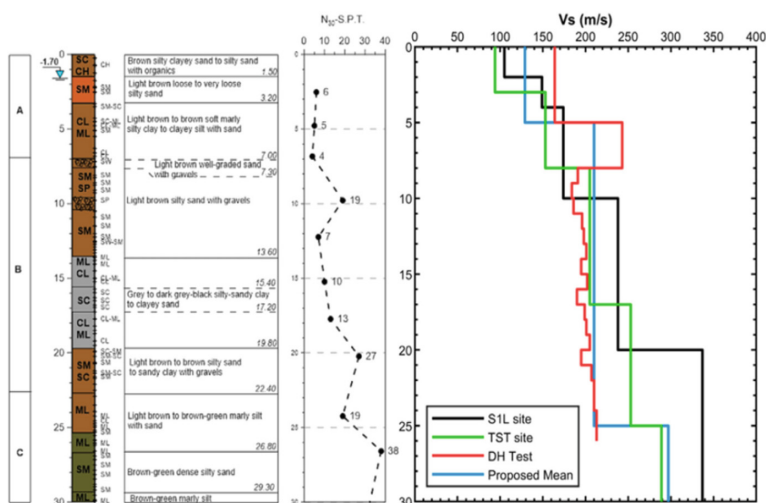

Fig. 11. Soil stratigraphy and V_s vs z profile underneath the Europroteas structure.

Many instruments were used to record the response of the structure, the foundation, the GRM layer, and the soil in the vertical "z" direction and the two horizontal NS "N" and EW "E" directions (Fig. 12). The structure was instrumented with accelerometers installed: on the roof, both along the direction of shaking (that is the "N" direction) and at the opposite corners of the roof to capture possible out-of-plane motion; and on the foundation, forming a cross shape to capture its translational, rocking, and possible out-of-plane motion. Seismometers were located on the soil surface, both along the loading axis and on the perpendicular axis. The distance between those close to the structure was defined at 0.50 m = B/6, where B is the foundation width. The most distant instrument was installed at 5 m = 5B/3. Finally, a shape-acceleration array equipped with sensors every 0.15 cm was installed immediately below the geometrical center of the foundation to capture the GRM layer response. Accelerometers were buried under the foundation to monitor the full response of the GRMs. More details about the tests can be found in [45].

The experimental test was simulated using the FEM MIDAS FEA-NX code [50]. A comparison between the experimental and the FEM results allowed the authors to validate the FEM model and to use it in future predictions of real case histories. Figure 13
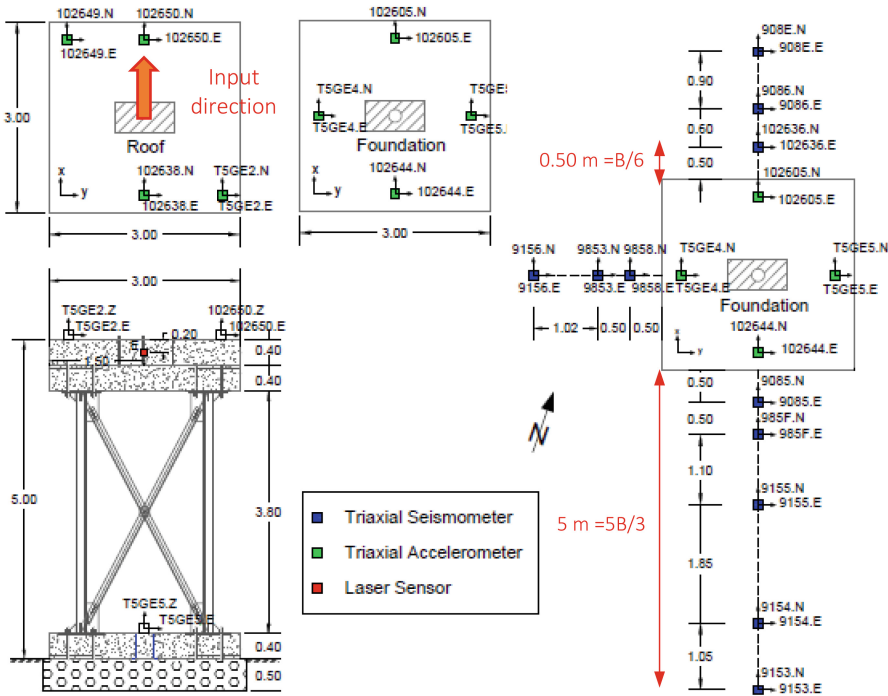
Fig. 12. Plan view of the instrumentation used for the full-scale tests on the Europroteas structure, including GRMs at the base.

shows the mesh, which was 20 m in total depth (z-direction), 30 m long (x-direction, corresponding to the input direction) and 20 m wide (y-direction). Free field edges were defined along the lateral boundaries of the 3D model. 3D solid elements were used, and the sizes of the mesh elements were fixed so as to reproduce all the waveforms of the whole frequency range under examination. To model foundation uplifting and sliding phenomena, contact surfaces were used between the foundation and the GRMs. A linear-elastic behavior was assumed for the structure, while a hardening soil model was used for the soil and the GRMs. The 3D model was fixed at the base, and a harmonic displacement input was applied to the roof in the x-direction according to the shaker force F used during the tests.

Due to a lack of space, only some experimental and numerical results are presented in this paper. Figure 14 shows the experimental results regarding the motion decay along with the structure and soil in terms of maxima accelerations for the input frequencies equal to 2.5 Hz and 4 Hz, close to the resonance frequencies of the GSI-structure systems. For the input frequency $f = 2.5$ Hz, the highest maxima accelerations occurred in the presence of GRM 70/30 since resonance occurs for this frequency. Comparing the acceleration at the roof with that at the foundation, an almost constant decrease was found for all the GRMs. However, the accelerations differed considerably for GRM 100/10 and GRM 90/10 on the one hand and GRM 70/30 on the other. It depends on the input frequencies and the natural frequencies of the system. Similar results were obtained comparing the accelerations at the foundation and the soil surface (0.5 m from

the foundation). Finally, moving through the soil surface (from 0.5 m up to 2.0 m from the foundation), there was a different acceleration decrease: the small value obtained for GRM 100/0 may be due to its higher stiffness and more negligible damping. Similar results were found for the input frequency f = 4 Hz. It is important to stress the critical decrease in the acceleration when going from the foundation to the soil next to the foundation, especially in the case of GRM 70/30. This confirms the supposed ability of the recycled rubber included in GRMs to trap the dynamic wave, thus avoiding its passage from the foundation to the soil. So, the GSI of the structure, represented by the GRM layer underneath the foundation, is optimized by increasing the rubber content of the soil rubber mixture up to 30% per mixture weight.

For all the GRMs used and the input frequencies 2.0, 2.5, 3.0, 4.0, 5.0 and 7.0 Hz, Figs. 15 and 16 report a comparison between the experimental results and the numerical ones in terms of acceleration in the "N" direction at the roof and the foundation, respectively. The experimental results refer to accelerometer N. 102650 on the roof and to accelerometer N. 102605 on the foundation. The figures generally show an excellent comparison between the experimental results and the numerical ones. Some moderate differences exist at the foundation for GRM 70/30 and the input frequency equal to 7.0 Hz and GRM 100/0 and GRM 90/10 when the input frequency is $\geq$ 4.0 Hz. It is important to stress that 7.0 Hz is the estimated third natural frequency of the structure resting on GRM 70/30, and 4.0 Hz is very close to the estimated first natural frequencies of the structure resting on GRM 100/0 and GRM 90/10. When approaching the resonance frequency, some differences between experimental and numerical results are unavoidable. From Figs. 15 and 16, it is also possible to observe an increase in the signal for the input frequencies around 2.5 Hz and 7.0 Hz for GRM 70/30 and around 4.0 Hz for GRM 100/0 and GRM 90/10, according to the estimated natural frequencies of the GSI-structure systems previously discussed.

Focusing on GRM 70/30 and the input frequency of 2.5 Hz, Fig. 17 reports a comparison between the experimental results and the numerical ones for the roof, the foundation and the soil. The numerical modelling allowed us to capture the results in the structure and the soil near the structure very well. Some discrepancies exist considering soil-structure distances greater than 1.00 m; see the velocity transducers N. 985F, N. 9086 and N. 908E. However, the numerical simulation completely captures the reduction of the signal from the roof (source point) to the foundation and from the foundation to the soil next to the structure.

Finally, Fig. 18 reports the experimental and numerical results in terms of acceleration response factor R_a versus the input frequency. R_a was calculated as the ratio of the recorded acceleration on the roof over the shaker force divided by the superstructure mass. The experimental results refer to accelerometer N. 102650 in the "N" direction. It is possible to observe that the frequency of the system shifted to 4 Hz for both GRM 100/0 and GRM 90/10, but the values of R_a using GRM 90/10 were slightly smaller than those using GRM100/0, indicating a modest increase in the damping due to the presence of rubber in GRM 90/10. The resonant frequency of the structure resting on GRM 70/30 presented a pronounced shift to 2.5 Hz, underlining the strong effect of the rubber on the stiffness reduction of the GSI-structure system. Considering the structure resting on GRM 70/30 the R_a values were much lower than those for the structure resting on GRM

100/0 and GRM 90/10, indicating a significant increase in the damping due to the greater rubber content. The numerical results precisely confirm the experimental ones.
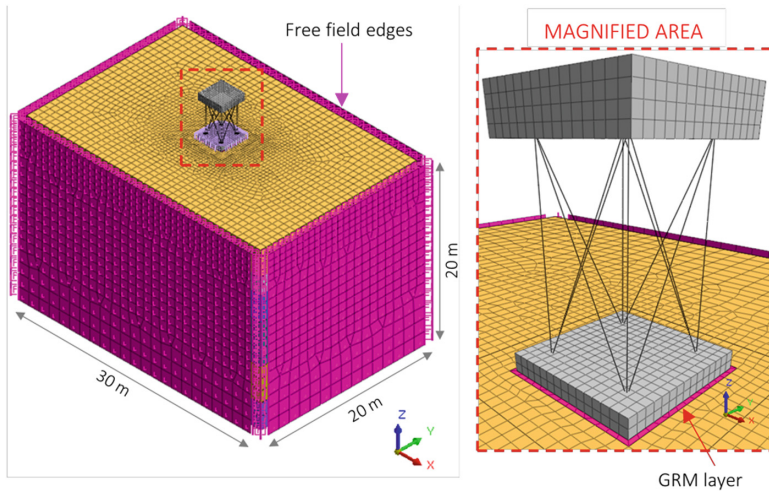

Fig. 13. Mesh made with the FEM MIDAS FEA-NX code for simulating the full-scale tests on the Europroteas structure.
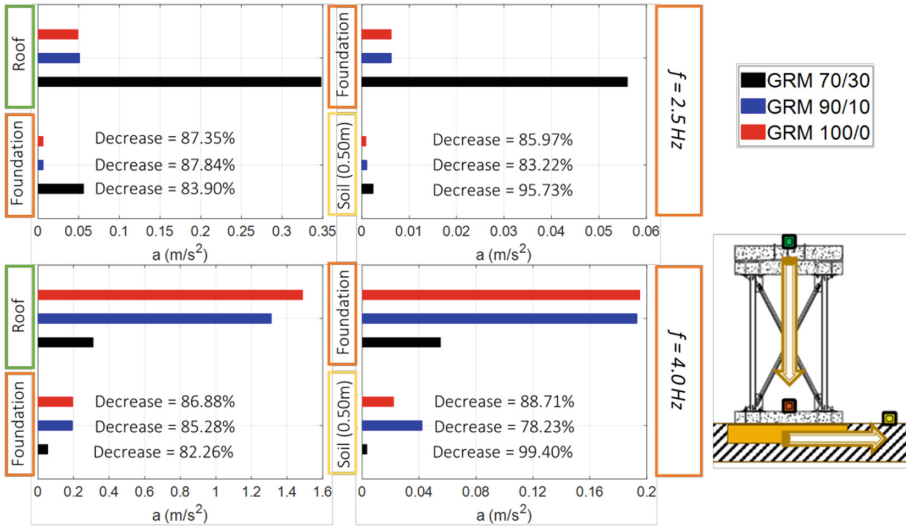

Fig. 14. Maxima acceleration decay along the structure and on the soil recorded during the Europroteas tests for input frequencies equal to 2.5 Hz and 4.0 Hz.
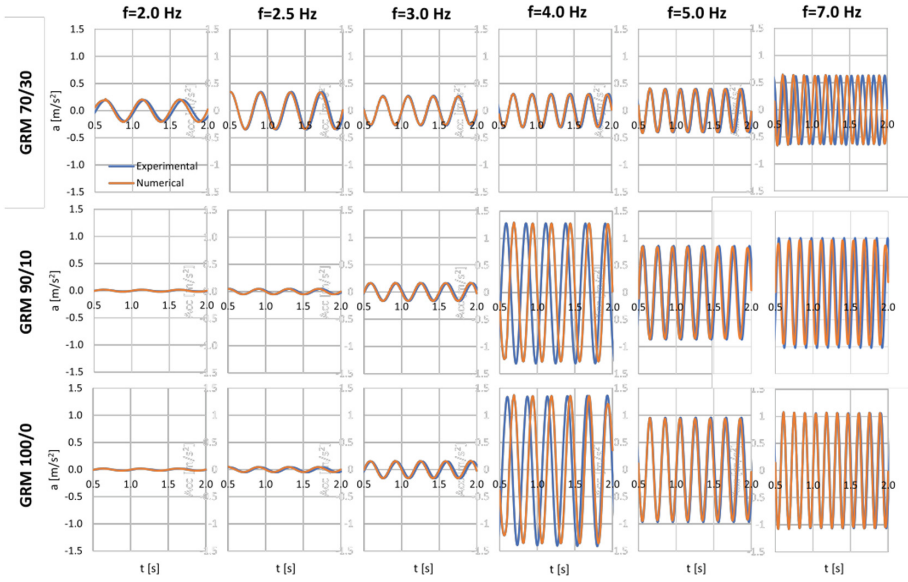
Fig. 15. Experimental versus numerical accelerations on the roof along the "N" direction.
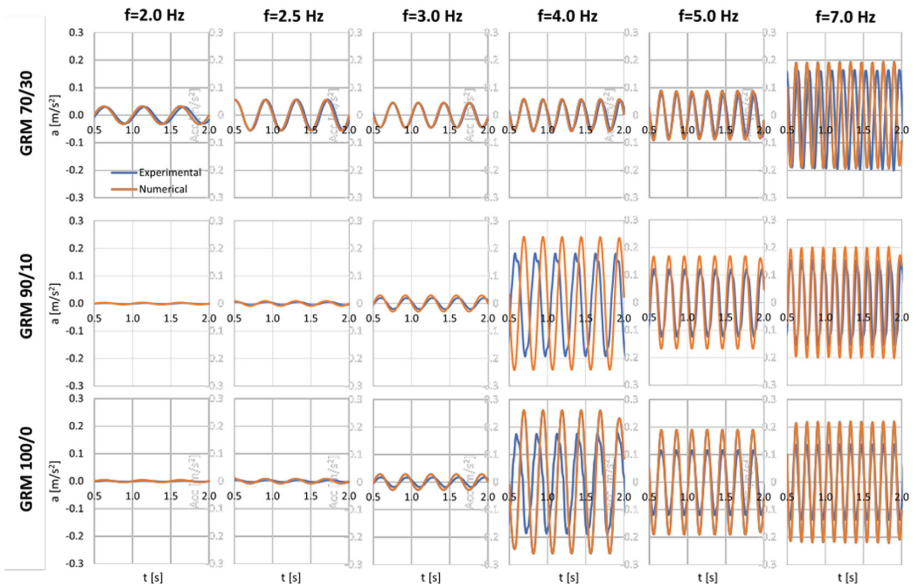

Fig. 16. Experimental versus numerical accelerations at the foundation along the "N" direction.
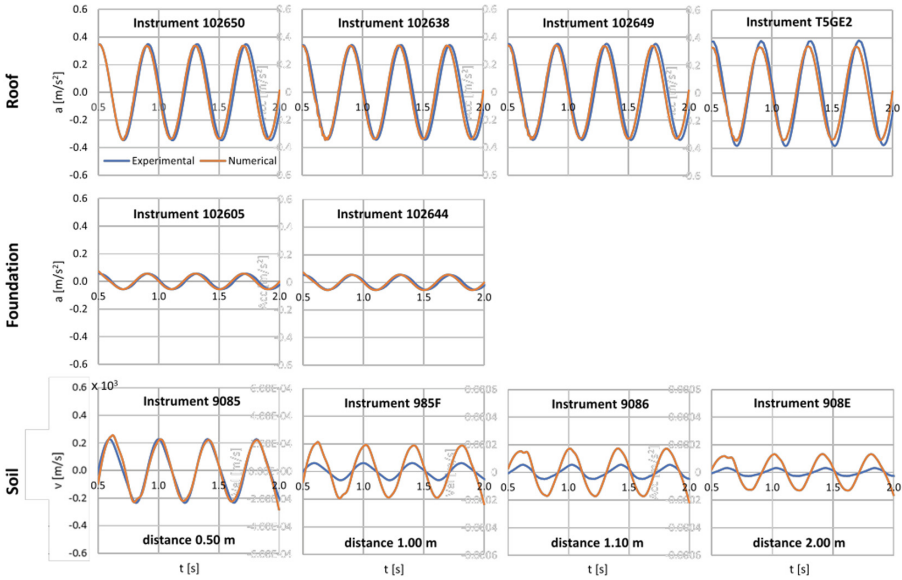
Fig. 17. Comparison between the experimental and numerical results for the soil-structure system, including GRM 70/30 and an input frequency equal to 2.5 Hz ("N" direction).
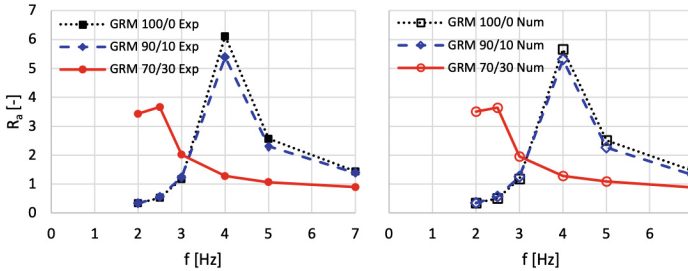

Fig. 18. Experimental and numerical acceleration response factors R_a versus the input frequency ("N" direction).

5 Conclusions

The seismic retrofitting of historic structures and the safeguarding of the ecosystem are two of the most pressing challenges at the present moment in time. Europe has a rich heritage of old structures of great architectonic and historical value, which unfortunately are characterized by a high seismic vulnerability and are located in areas with a medium-high seismic hazard. At the same time, waste management is pushing for waste to be transformed into valuable resources.

This paper presents two levels of analysis for investigating structural seismic risk, including the fundamental presence of the soil. The first level is based on sophisticated local site response analyses. The second level is based on the investigation of fully

coupled soil-structure systems, which most closely reflect the actual structural configurations. These levels of analysis are discussed with reference to two interesting case histories.

Finally, the first experimental campaign performed on a full-scale prototype structure resting on gravel-rubber mixtures (GRM) and the related FEM simulation are presented. Rubber grains are manufactured from scrap tyres, and the aim is to test GRMs as a geotechnical seismic isolation (GSI) that combine seismic risk mitigation and ecosystem protection.

The main results can be summarized as follows:

– LSR analyses allow us to produce seismic microzonation maps, based on real soil profiles and including soil nonlinearity. LSRs are generally performed in free-field conditions. The critical role played by the soil must be investigated in the time and frequency domains. The case history discussed reports the most severe responses for the inputs characterized by low peak values of amplitude and predominant frequencies close to the natural frequencies of the soil. Possible resonant phenomena in the soil can be appropriately captured only through accurate LSR analysis. An approximate evaluation of the soil filtering effect can give a wrong evaluation of the real inputs affecting the structures.
– DSSI analyses of fully coupled soil-structure systems often furnish values of spectral acceleration higher than those given by the technical regulations or obtained by LSR analysis in free-field conditions for periods higher than 0.7 s, which are typical of structures with an unrealistic fixed base. Nowadays, DSSI analyses should be used much more as part of routine design, recognizing the inadequacy of some of the simplistic assumptions that have been imposed in the past for reasons of calculational expediency.
– The experimental tests on the full-scale prototype structure resting on GRMs, confirm the supposed ability of the recycled rubber included in the GRMs to trap the dynamic wave, thus avoiding its passage from the foundation to the soil and vice versa. The GSI of the structure, represented by the GRM layer underneath the foundation, is optimised by increasing the rubber content of the gravel-rubber mixture up to 30% per mixture weight.

References

1. Caruso, S., Ferraro, A., Grasso, S., Massimino, M.R.: Site response analysis in eastern Sicily based on direct and indirect vs measurements. In: 1st IMEKO TC4 International Workshop on Metrology for Geotechnics, MetroGeotechnics 2016 Proceedings, pp. 115–120 (2016)

2. Ferraro, A., Grasso, S., Massimino, M.R.: Site effects evaluation in Catania (Italy) by means of 1-D numerical analysis. Ann. Geophys. **61**(2), SE224 (2018)
3. Pagliaroli, A., et al.: Site response analyses for complex geological and morphological conditions: relevant case-histories from 3rd level seismic microzonation in Central Italy. Bull. Earthq. Eng. **18**(12), 5741–5777 (2019). https://doi.org/10.1007/s10518-019-00610-7
4. Pitilakis, K., Riga, E., Anastasiadis, A.: Design spectra and amplification factors for Eurocode 8. Bull. Earthq. Eng. **10**(5), 1377–1400 (2012)
5. Andreotti, G., Famà, A., Lai, C.G.: Hazard-dependent soil factors for site-specific elastic acceleration response spectra of Italian and European seismic building codes. Bull. Earthq. Eng. **16**(12), 5769–5800 (2018). https://doi.org/10.1007/s10518-018-0422-9
6. Tropeano, G., Soccodato, F.M., Silvestri, F.: Re-evaluation of code-specified stratigraphic amplification factors based on Italian experimental records and numerical seismic response analyses. Soil Dyn. Earthq. Eng. **110**, 262–275 (2018)
7. Aimar, M., Ciancimino, A., Foti, S.: An assessment of the NTC18 stratigraphic seismic amplification factors. Rivista Italiana di Geotecnica **1**, 5–21 (2020)
8. Paolucci, R., et al.: Checking the site categorization criteria and amplification factors of the 2021 draft of Eurocode 8 Part 1–1. Bull. Earthq. Eng. **19**(11), 4199–4234 (2021). https://doi.org/10.1007/s10518-021-01118-9
9. Gazetas, G.: Foundation vibrations. In: Fang, H.-Y. (ed.) Foundation Engineering Handbook, 2nd edn. Chapman and Hall, New York (1991)
10. EN 1998-5: Eurocode 8: Design of structures for earthquake resistance - Part 5: Foundations, retaining structures and geotechnical aspects. European Committee for Standardization, Brussels (2004)
11. FEMA: NEHRP Recommended Seismic Provisions for New Buildings and Other Structures. Building Seismic Safety Council of the National Institute of Building Sciences for the Federal Emergency Management Agency, Washington, DC, USA (2009)
12. Massimino, M.R., Biondi, G.: Some experimental evidences on dynamic soil-structure interaction. In: Papadrakakis, M., Papadopoulos, V., Plevris, V. (eds.) 5th ECCOMAS Thematic Conference on Computational Methods in Structural Dynamics and Earthquake Engineering Proceedings, COMPDYN 2015, Crete Island, Greece, 25–27 May 2015. Code 113952, pp. 2761–2774 (2015). ISBN 978-960-99994-7-2
13. Massimino, M.R., Abate, G., Grasso, S., Pitilakis, D.: Some aspects of DSSI in the dynamic response of fully-coupled soil-structure systems. Rivista Italiana di Geotecnica **2019**(1), 44–70 (2019)
14. Massimino, M.R., Abate, G., Corsico, S., Louarn, R.: Comparison between two approaches for nonlinear FEM modelling of the seismic behaviour of a coupled soil-structure system. Geotech. Geol. Eng. **37**(3), 1957–1975 (2019)
15. Maugeri, M., Abate, G., Massimino, M.R.: Soil-Structure Interaction for Seismic Improvement of Noto Cathedral (Italy). Geotech. Geol. Earthq. Eng. **16**, 217–239 (2012)
16. Abate, G., Massimino, M.R.: Dynamic soil-structure interaction analysis by experimental and numerical modelling. Rivista Italiana di Geotecnica **50**(2), 44–70 (2016)
17. Abate, G., Massimino, M.R., Romano, S.: Finite element analysis of DSSI effects for a building of strategic Importance in Catania (Italy). Procedia Eng. **158**, 374–379 (2016)
18. Abate, G., Bramante, S., Massimino, M.R.: Innovative seismic microzonation maps of urban areas for the management of building heritage: a Catania case study. Geosciences **10**(12), 1–22 (2020)
19. Karatzetzou, A., Pitilakis, D.: Modification of dynamic foundation response due to soil-structure interaction. J. Earth. Eng. **22**(5), 861–880 (2017)
20. NTC 2018. New technical standards for buildings, Official Journal of the Italian Republic February 20th 2018 (in Italian) (2018)

21. Amendola, C., de Silva, F., Vratsikidis, A., Pitilakis, D., Anastasiadis, A., Silvestri, F.: Foundation impedance functions from full-scale soil-structure interaction tests. Soil Dyn. Earthq. Eng. **141**, 106523 (2021)

22. Brunelli, A., et al.: Numerical simulation of the seismic response and soil–structure interaction for a monitored masonry school building damaged by the 2016 Central Italy earthquake. Bull. Earthq. Eng. **19**(2), 1181–1211 (2020). https://doi.org/10.1007/s10518-020-00980-3

23. Mylonakis, G., Gazetas, G.: Seismic soil-structure interaction: beneficial or detrimental? J. Earthq. Eng. **4**(3), 277–301 (2000)

24. D'Amato, M., Gigliotti, R., Laguardia, R.: Seismic isolation for protecting historical buildings: a case study. Front. Built Environ. **5**, 87 (2019). https://doi.org/10.3389/fbuil.2019.00087

25. Gatto, M.P.A., Lentini, V., Castelli, F., Montrasio, L., Grassi, D.: The use of polyurethane injection as a geotechnical seismic isolation method in large-scale applications: a numerical study. Geosciences **11**(5), 201 (2021)

26. Micozzi, F., Scozzese, F., Ragni, L., Dall'Asta, A.: Seismic reliability of base isolated systems: sensitivity to design choices. Eng. Struct. **256**(5), 114056 (2022)

27. Anastasiadis, A., Senetakis, K., Pitilakis, K.: Small-strain shear modulus and damping ratio of sand-rubber and gravel-rubber mixtures. Geotech Geol. Eng. **30**, 363–382 (2012)

28. Tsang, H.H., Lo, S.H., Xu, X., Sheikh, M.N.: Seismic isolation for low-to-medium-rise buildings using granulated rubber-soil mixtures: numerical study. Earthq. Eng. Struct. Dynam. **41**, 2009–2024 (2012)

29. Tsang, H.H., Pitilakis, K.: Mechanism of geotechnical seismic isolation system: analytical modeling. Soil Dyn. Earthq. Eng. **122**, 171–184 (2019)

30. Tsang, H., Tran, D., Hung, W., Pitilakis, K., Gad, E.F.: Performance of geotechnical seismic isolation system using rubber-soil mixtures in centrifuge testing. Earthq. Eng. Struct. Dyn. **50**, 1271–1289 (2020). https://doi.org/10.1002/eqe.3398

31. Pistolas, G.A., Pitilakis, K., Anastasiadis, A.: A numerical investigation on the seismic isolation potential of rubber/soil mixtures. Earthq. Eng. Eng. Vib. **19**(3), 683–704 (2020). https://doi.org/10.1007/s11803-020-0589-3

32. Tasalloti, A., Chiaro, G., Murali, A., Banasiak, L., Palermo, A., Granello, G.: Recycling of end-of-life tires (ELTs) for sustainable geotechnical applications: a New Zealand perspective. Appl. Sci. **11**(17), 7824 (2021)

33. Tasalloti, A., Chiaro, G., Banasiak, L., Palermo, A.: Experimental investigation of the mechanical behaviour of gravel-granulated tyre rubber mixtures. Constr. Build. Mater. **273**, 121749 (2021)

34. Chiaro, G., Tasalloti, A., Chew, K., Vinod, J.S., Allulakshmi, K.: Macro and microscale engineering response of rigid-soft gravel-rubber inclusions: insights from detailed laboratory and DEM numerical investigations. In: Gupta, A.K., Shukla, S.K., Azamathulla, H. (eds.) Advances in Construction Materials and Sustainable Environment. LNCE, vol. 196, pp. 11–27. Springer, Singapore (2022). https://doi.org/10.1007/978-981-16-6557-8_2

35. Boschi, E., Guidoboni, E, Ferrari, G., Mariotti, D., Valensise, G., Gasperini, P.: Catalogue of strong Italian earthquakes from 461 b.c. to 1997. Ann. Geophys. **3**(4) (2000)

36. Camassi, R., Stucchi, M.: - NT4.1, a parametric catalogue of damaging earthquakes in the Italian area (release NT4.1.1). GNDT, Milano, Italy (1998)

37. Bottari, A., Saraò, A., Teramo, A., Termini, D., Carveni, P.: The January 11th, 1693 South-Eastern Sicily earthquake: macroseismic analysis and strong motion modelling at Noto. In: Maugeri, M., Nova, R. (eds.) Geotechnical Analysis of the Seismic Vulnerability of Historical Monuments, Pàtron, Bologna (2003)

38. Cavallaro, A., Maugeri, M.: Site characterisation by in-situ and laboratory tests for the microzonation of Noto. In: Maugeri, M., Nova, R. (eds.) Geotechnical Analysis of the Seismic Vulnerability of Historical Monuments, Pàtron, Bologna (2003)

39. Frenna, S.M., Maugeri, M.: The GEODIN code for the analysis of the soil seismic response. In: IX Convegno Italiano di Meccanica Computazionale Proceedings, Catania, 20–22 June 1995, pp. 145–148 (1995). (in Italian)
40. Campoccia, I., Massimino, M.R.: Grade-3 microzonation at Noto. In: Maugeri, M., Nova, R. (eds.) Geotechnical Analysis of Seismic Vulnerability of Monuments and Historical Sites, pp. 257–286 (2003). ISBN 88-555-2755-X
41. EN 1998-1: Eurocode 8: Design of structures for earthquake resistance - Part 1: General rules, seismic actions and rules for buildings. European Committee for Standardization, Brussels (2004)
42. NTC 2008: D.M. 14/01/08 - New technical standards for buildings, Official Journal of the Italian Republic, January 14th 2008 (2008). (in Italian)
43. Grasso, S., Laurenzano, G., Maugeri, M., Priolo, E.: Seismic response in Catania by different methodologies. Adv. Earthq. Eng. **14**, 63–79 (2005)
44. Massimino, M.R., Abate, G., Corsico, S., Grasso, S., Motta, E.: Dynamic behaviour of coupled soil-structure systems by means of FEM analysis for the seismic risk mitigation of INGV building in Catania (Italy). Ann. Geophys. **61**(2), SE216 (2018). https://doi.org/10.4401/ag-7739
45. Pitilakis, D., et al.: Large-scale field testing of geotechnical seismic isolation of structures using gravel-rubber mixtures. Earthq. Eng. Struct. Dynam. **2021**, 1–20 (2021). https://doi.org/10.1002/eqe.3468
46. Abate, G., Gatto, M., Massimino, M.R., Pitilakis, D.: Large scale soil-foundation-structure model in Greece: dynamic tests vs FEM simulation. In: Papadrakakis, M., Fragiadakis, M. (eds.) 6th Eccomas Thematic Conference on Computational Methods in Structural Dynamics and Earthquake Engineering Proceedings. COMPDYN 2017, Rhodes Island, Greece, 15–17 June 2017, pp. 1347–1359 (2017). ISBN 978-618828441-8. https://doi.org/10.7712/120117.5497.16830
47. Pitilakis, D., Rovithis, E., Anastasiadis, A., Vratsikidis, A., Manakou, M.: Field evidence of SSI from full-scale structure testing. Soil. Dyn. Earthq. Eng. **112**, 89–106 (2018)
48. Vratsikidis, A., Pitilakis, D.: Full-scale free- and forced-vibration experiments at the EuroProteas SSI facility: experimental data exploitation. In: 16th European Conference on Earthquake Engineering Proceedings, Thessaloniki (2018)
49. Pitilakis, K., Raptakis, D., Lontzetidis, K., Tika-Vassilikou, T., Jongmans, D.: Geotechnical and geophysical description of EURO-SEISTEST, using field, laboratory tests and moderate strong motion recordings. J. Earthq. Eng. **3**, 381–409 (1999)
50. Midas FEA NX – 2022 (v.1.1); CSPFEA—Engineering Solutions: Este, Italy (2022)